DOE/ER/14105--3

DE93 005928

PROGRESS REPORT

Title : Photoinduced Electron Transfer Reactions in Zeolite Cages

Duration : 1/15/90 - 8/1/92

Grant Number : DE-FG02-90ER14105

Principal Investigator : Dr. Prabir K. Dutta
Department of Chemistry
The Ohio State University
Columbus, Ohio 43210

Progress Report

Over the past two and a half years, our research has been primarily in the field of photochemical reactions in zeolites. We have also examined a support that complements the studies done with zeolites. These materials belong to the class of layered double metal hydroxides. The five publications that have resulted from these studies so far are included in the Appendix and also listed at the end of this section. In this progress report, we have mostly focused on unpublished results that will form the material for publications in the near future. This report summarizes the work in the area of zeolites followed by the layered double hydroxides.

(a) **Zeolites**:

Zeolites are crystalline aluminosilicates of general composition $M_{x/n}[(AlO_2)_x(SiO_2)_y].z\ H_2O$, where the M^{n+} cations preserve the electrical neutrality of the negative aluminosilicate framework. Typically, Na^+ is the neutralizing cation and its content is the same as the Al present in the framework. The arrangement of the Si, Al and O atoms gives rise to distinct topological structures, about 50 of which are known. In our studies, we have exclusively focused on the faujasitic zeolite, the structure of which is shown below.

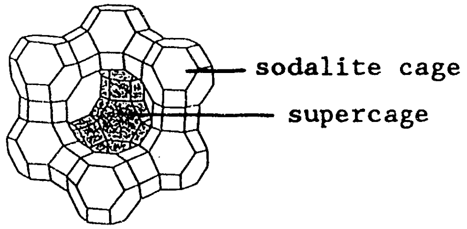

The system of choice was $Ru(bpy)_3^{2+}$. The photochemical and photophysical properties of this molecule has been extensively studied, and provides an excellent model system to evaluate the influence of zeolites. Interestingly enough, this molecule can be synthesized inside the pores of zeolite Y, and remains trapped though it can communicate with the outside environment through the twelve-membered 7 Å ring openings. We have examined both the structural and photochemical properties of the $Ru(bpy)_3^{2+}$-zeolite Y system, and the results are detailed below.

(a) **Structural Studies**:

The major conclusion of our previous studies on the structural aspects of $Ru(bpy)_3^{2+}$-zeolite Y can be summarized as:

(1) $Ru(bpy)_3^{2+}$ can be synthesized in zeolite Y supercages in high purity and yields.

(2) Even though the ~12 Å molecule is encapsulated in 13 Å supercages, the properties of $Ru(bpy)_3^{2+}$ in hydrated zeolite Y at low loadings (~1 in 15 supercages) resembles an aqueous solution of $Ru(bpy)_3^{2+}$. Though much of the water is excluded from the zeolite cage in which the $Ru(bpy)_3^{2+}$ is present, the continuous intracrystalline water that surrounds the cage and extends into it through the 12, 6, and 4 membered aluminosilicate rings of the supercage wall provide a hydrated environment.

(3) Dehydration alters the energetics and lifetime of the MLCT state and is proposed to arise from interaction of the framework electrostatic fields with the dipolar MLCT state.

(4) Packing of $Ru(bpy)_3^{2+}$ molecules in the zeolite supercages can be varied from very low loadings (1 per 100 supercages) to saturation loadings of 1 per supercage. At these highest loadings, molecules share neighboring cages. This leads to strong interactions between the coordinated bpy ligands through the 7Å cages, and is manifested in changes of both ground and excited state properties. Emission quenching of neighboring $Ru(bpy)_3^{2+}$ occur by the Perrin mechanism with a sphere of action radius of 13 Å. At high excitation energies, evidence for triplet-triplet quenching is also found to occur.

(b) **Photochemical Studies**:

Photoinduced electron transfer between entrapped $Ru(bpy)_3^{2+}$ and methylviologen (MV^{2+}) in neighboring supercages has been examined. The communication between the donor and acceptor has to occur through the 7Å ring openings. Though the $Ru(bpy)_3^{2+}$ is trapped, the MV^{2+} can migrate through the zeolite network.

(1) Evidence for photoelectron transfer is provided by time resolved Raman spectroscopy, which shows the formation of $MV^{+\bullet}$ within 15ns.

(2) Two pathways are observed for the decay of the violgen radical cation. The first is a rapid back electron transfer to Ru^{3+} over a period of tens of microseconds.

(3) Another pathway, though quite inefficient leads to stabilization of radical $MV^{+\bullet}$ species. We have proposed that as the MV^{2+} diffuse through the zeolite system, particular stacking orientations are set up, such that electrons can hop across viologens, thus resulting in spatial charge separation, as shown below schematically.

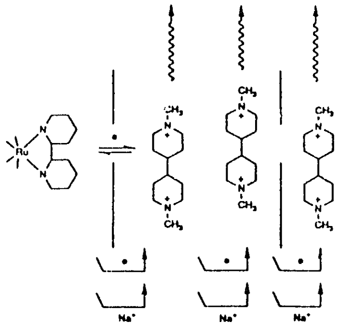

(4) The motion of the co-cation (e.g. Na^+ for Na-Y or Li^+ for Li-Y), necessary to balance the charge as the photoelectron migrates influences the rate of the charge separation process.

The following results have not yet been published. There are two aspects of this photochemical reaction that we are addressing. The first deals with the fact that in order to utilize the charge separated products for further chemistry, we need to remove one of the photoproducts from the zeolite, preferably into solution. Since the $Ru(bpy)_3^{2+}$ is trapped, it needs to be the viologen cation. The second aspect is that the yield of the charge separation process needs to be enhanced.

(5) In order to remove the $MV^{+\bullet}$ from the zeolite, we have taken advantage of the ion-exchange properties of zeolites, as shown below schematically.

$$\boxed{Ru(bpy)_3^{3+} \;||\; MV^{+\cdot}} + Na^+\,(soln) \rightarrow \boxed{Ru(bpy)_3^{3+} \;||\; Na^+} + MV^{+\cdot}\,(soln)$$

The Na^+/MV^{2+} ratio of the solution influences the rate of appearence of the viologen radical cation in solution (shown below). The figure to the left is the electronic spectra of the solution above a $Ru(bpy)_3^{2+}$-zeolite pellet as it is being photolyzed by visible light. It is clear that $MV^{+\bullet}$, as evidenced by bands at 390 and 610 nm is being formed in solution. The curves on the right compare the $MV^{+\bullet}$ radical yield as a function of MV^{2+} concentration in solution.

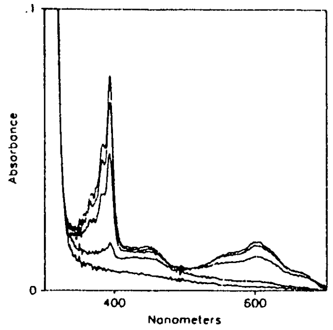

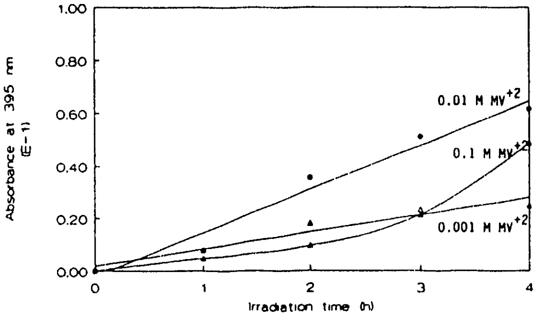

(6) Another strategy to remove the photoinduced charge from the zeolite is to transfer it to a species in the surrounding solution across the zeolite interface. By choosing neutral viologen molecules in solution as acceptors, it is ensured that they will not replace the ion exchanged viologen inside the zeolite. Upon accepting the electron from the zeolite, the viologen in solution becomes negatively charged and is repelled by the zeolite framework. Also, in the choice of the two viologens, it is essential that the driving force for electron transfer be directed from the zeolite to the solution. In the two cases that we have examined, BV^{2+} (benzylviologen) or MV^{2+} was within the zeolite and PVS (propylviologen sulfonate) was in solution. The yields of PVS radical formed by photolysis are compared below for the two cases, and is considerably enhanced in the case of BV^{2+}.

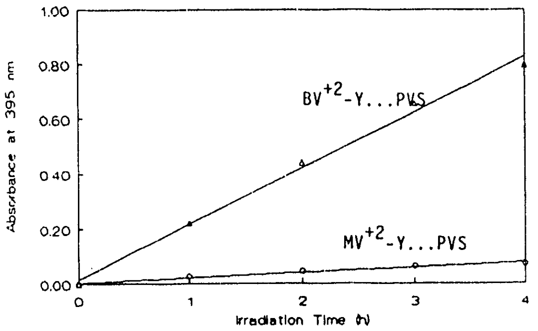

The E° of BV^{2+}(-0.33 v vs NHE) is higher than PVS (-0.40 V vs NHE) by 70 mV and electron transfer should not be expected because it is going uphill. Efficient electron transfer is only realized when BV^{2+} is packed as densely as possible in the supercages of zeolite Y. It is well known that the E° of the viologens decrease if there is any deviation from planarity of the benzene rings. We propose that in the highly packed BV^{2+}-Y, the steric constraints inside the supercages lead to puckering of the ring, thus resulting in decrease of reduction potential, making the electron transfer from intrazeolitic BV^{2+} to PVS in solution facile. The Raman spectra shown below compares BV^{2+} in solution with that in the zeolite and spectral changes confirm that structural alterations are occuring. Bands at 1297 (inter-ring C-C stretch) and 1645 cm^{-1} shift to 1301 and 1649 cm^{-1}, respectively.

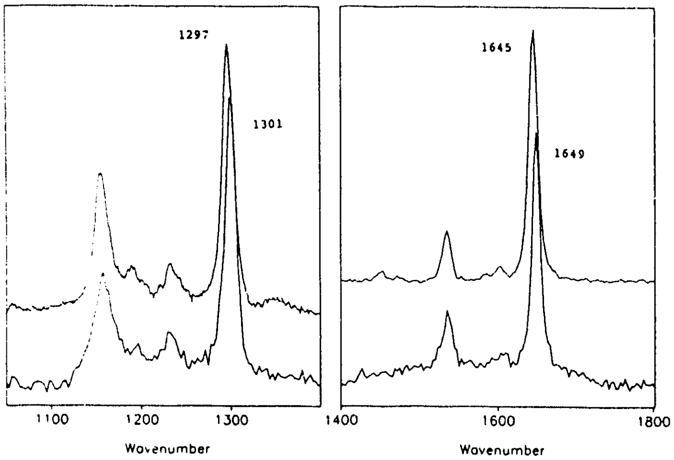

Electrochemical studies of highly loaded BV^{2+} are in progress to determine its reduction potential in the zeolite. In contrast, the MV^{2+}-zeolite Y does not show an enhanced electron transfer to PVS. The MV^{2+} cations are about the length of the supercages, and even at the highest loadings of 2 molecules per supercage do not appear to undergo structural changes which alter the reduction potential. In the case of BV^{2+}, the benzyl groups force the viologen to span more than a supercage, thereby leading to distortion. Further studies aimed at understanding and optimizing this system are discussed in the research plan.

There are two other studies that we have completed during this phase of the program that have a bearing on our future plans. These include a quantitative evaluation of the zeolite as a solvent and generation of small metal clusters in zeolite cages.

The intracrystalline space in the zeolite is akin to a solvent and description of this space in terms of solvent like properties is appropriate. In particular, we have focused on how the solvent properties of zeolites change as a function of Si/Al ratio. We consider this particularly important since we plan to examine photoelectron transfer in zeolites as a function of Si/Al ratio. Borrowing from physical organic chemistry, we used salicylideneaniline, a solvatochromic molecule for characterizing Na-Y. It was found that the empty zeolite cages are best described as an α solvent, which indicates that the framework interacts with molecules via acid-base interactions. The zeolite as a solvent compares well with hydroxylic solvents. It was found that the α value of the zeolite increased with Si/Al ratio to reach a maximum around 8, follwed by a decrease at higher Si/Al values. The acidic functionalities in a zeolite are the Na^+ cations, whereas the framework oxygens act as bases. We propose to examine how this changing acid-base behavior as a function of Si/Al ratio influences the excited state of $Ru(bipyrazine)_3^{2+}$.

Another area that we have examined is the photolysis of metal carbonyls in zeolites in order to generate small metal clusters. As described below, we plan to examine the interaction of photoexcited $Ru(bpz)_3^{2+}$ with small metal clusters. The zeolite cages, by virtue of their constrained geometry allows for the creation and entrapment of small metal clusters. However, generating and characterizing these clusters is a nontrivial problem. We have shown that it is possible to generate atomic Fe by pulsed laser photolysis of $Fe(CO)_5$ and will adapt this procedure to the formation of small Ru clusters.

(b) **Layered Metal Hydroxides:**

In developing novel architecture for intrazeolitic photochemical electron transfer systems, the difficulty faced with the zeolitic system is that molecules larger than~13 Å cannot be accomodated in its cages. Other aluminophosphate and gallophosphate microporous materials are known with larger cage sizes but synthesis of metal complexes within their cages is difficult, due to lack of ion-exchange properties and thermal instabilities. There has been a recent patent report from Mobil, in which they claim cavity sizes in excess of 20 Å. We are investigating the possibility of use of these materials. Another problem with zeolites is that only cationic compounds can readily be assembled in its cages from aqueous solutions. These factors have led us to explore other hosts in which larger sensitizer molecules such as porphyrins, phthalocyanines or derivatized Ru polypyridyl complexes can be introduced.

The material that we have done preliminary work on and shows promise are layered double metal hydroxides (LDH) of composition $LiAl_2(OH)_6^+ X^-$. The metal hydroxide layer containing Li and Al is cationic and in order to maintain charge neutrality anions (X^-) are present in the interlayers. A schematic of such a structure is shown below. The accompanying electron micrograph show the typical dimensions of $LiAl_2(OH)_6^+$ (abbreviated henceforth as LiAl-LDH) particles to be about 2-3 μm in length and 0.1 μm in width. This corresponds to about 100 layers of metal hydroxide for each particle.

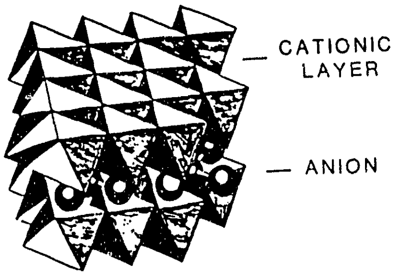

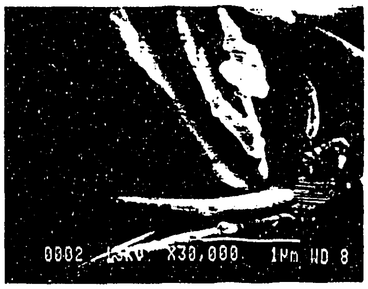

By choosing appropriate conditions, inorganic, organometallic and organic molecules can be introduced in the interlayer space. Our group has had considerable experience with synthesis and ion-exchange involving these materials. The interlayer space readily accomodates anionic species of varying dimensions by separation of the layers. The constraints of certain sizes of molecules is considerably relaxed. Design of the architecture of this interlayer space in order to promote photochemical charge separation has been the goal of this program. In this study, we have primarily dealt with the Li-Al layered double hydroxide.

Photoinduced redox reactions in organized media is an area of active research. In particular, organized assemblies involving surfactants and lipids in micelles, vesicles, microemulsions and liquid crystals allow for compartmentalization of reactants via hydrophobic-hydrophilic and electrostatic interactions. Below we discuss three areas that we have examined with the LDH materials. These include LDH as hosts for organized assembly of hydrophobic domains, incorporation of porphyrins and pyrene into the interlayer space and their photochemistry.

(1) Organized assemblies of hydrophobic domains are made by introducing into the interlayer long chain carboxylic acids $R(CH_2)_nCOOH$. Most of our work has focused on n—12,14 (myristic and palmitic acids, respectively), although longer chain acids can also be introduced. The arrangement and packing of the alkyl chains in the interlayers is controlled by interaction of the COO^- group with the positive charge on the metal hydroxide layer. By choosing a LDH as $LiAl_2(OH)_6^+$, wherein the spacing of the positive charges are 5Å apart, a dense and ordered packing of alkyl chains, similar to that of crystalline polyethylene is obtained. The orientation of the organic acid is readily determined by X-ray diffraction, as shown below. By replacing the chloride anion by myristate, the interlayer space has expanded from 3 to 21 Å, which is typical of the length of an all-trans myristic acid molecule.

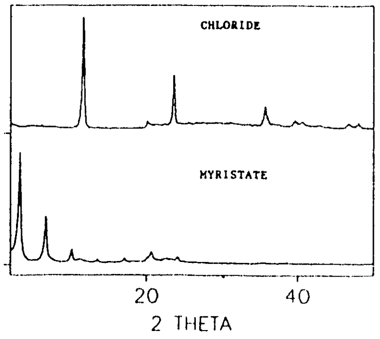

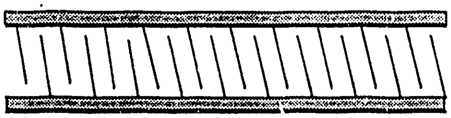

We have examined the packing and phase transitions in myristate-LDH by spectroscopic and thermal methods, and find characteristics similar to that for lipids in membranes. In membranes, the hydrophobic effect drives the aggregation of the alkyl chains, whereas in the LDH, the charge on the framework determines the aggregation. For example, if the charge density on the LDH is reduced, then the alkyl chains would be isolated from each other and probably lying in the interlayer with the alkyl chain parallel to the layer. Thus, these class of materials provides us with control of the packing of molecules in the interlayer space.

(2) Also present in the interlayer space along with the fatty acids are considerable amounts of ethanol which is used as the solvent for exchange (about 30 wt %). It is possible to introduce anionic chromophores into the interlayer space which disperse in these solvent pools. For example, zinc tetraphenylporphyrin sulfonate (ZnTPPS) can be incorporated into

myristate-LiAl-LDH from an ethanolic solution and the diffuse reflectance spectrum shown below is characteristic of the porphyrin.

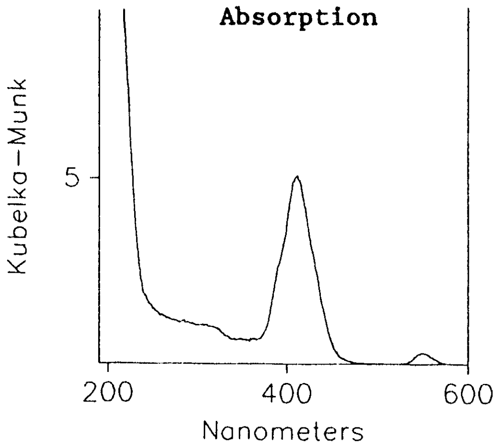

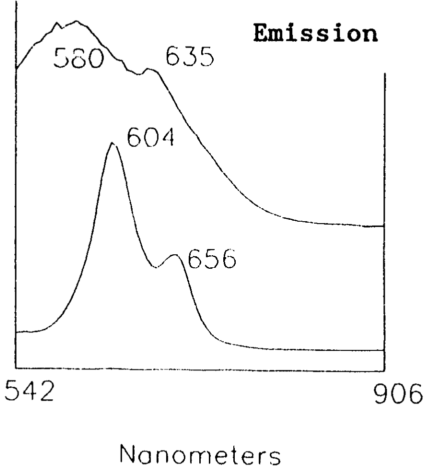

The uptake is controlled by adjusting the concentration of the porphyrin in solution and exhibits a saturation loading for the prophyrin. Neutral ZnTPP will not interacalate into the layers. The fluorescence spectra of the intercalated porphyrin exhibits bands at 580 and 635 nm as compared to 604 and 656 nm in dilute solution. Considering the negative charges on the sulfonate groups, it is likely that the porphyrins are located in the polar region of the material, near the metal hydroxide layer interface, rather than in the hydrophobic alkyl chains. Time resolved EPR spectra done by Prof. H. van Willigen suggests that the mobility of the porphyrin is quite restricted at room temperature, consistent with the binding to the cationic layer.

We have examined the steady state visible(400-640nm) photolysis of the ZnTPPS-LiAl-LDH with MV^{2+} in solution. An interesting observation was the steady state generation of $MV^{+\bullet}$in solution if the ethanol volume fraction exceeded fifty percent. From the absorption spectra below comparing the LDH based and homogeneous solution (porphyrin concentration- 10^{-6}M) in 50% water: ethanol, it is clear that $MV^{+\bullet}$ is being formed upon photolysis with the LDH sample.

Solution

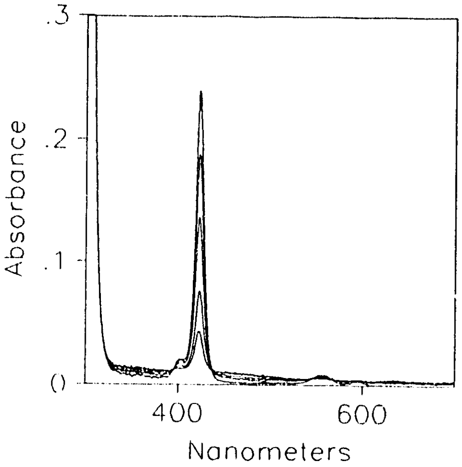

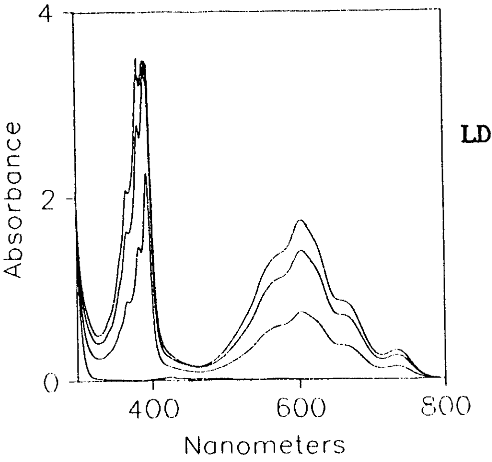

LDH

Analysis of the data based on different ethanol: H_2O mixtures indicate that the following process is occuring:

$$ZnTPPS^{4-} \xrightarrow{h\nu} {}^3ZnTPPS^{4-}$$

$${}^3ZnTPPS + MV^{2+} \rightarrow ZnTPPS^{3-} + MV^{+\bullet}$$

$$ZnTPPS^{3-} + C_2H_5OH \rightarrow ZnTPPS^{4-} + \text{other products}$$

The ability of C_2H_5OH to regenerate the $ZnTPPS^{4-}$ by acting as a sacrifical electron donor is known, though the mechanism is yet to be discerned. Also, the role of ethanol as a sacrificial electron donor is only observed in neat ethanol. Thus, we observe the viologen radical formation with the LDH system because the intercalated ZnTPPS is dispersed in the ethanol pools in the interlayers. It is necessary to have a certain fraction of ethanol in the external medium as a cosolvent with water so that MV^{2+} can approach the strongly hydrophobic myristate-LDH particles. This is supported by the observation that using a more hydrophobic acceptor such as heptylviologen (HV^{2+}), charge separation can be observed with lower co-solvent proportions of ethanol.

(3) The ZnTPPS in the interlayer remains at the metal hydroxide-carboxylate interface in the ethanol pools. We reasoned that it should be possible to disperse molecules in the middle of the fatty acid phase, if their hydrophobicity is large. There is considerable interest in the photoexcited triplet states of the polyaromatic hydrocarbons and their photochemical reactions. Long lifetimes and the spin-forbidden back electron transfer are advantages of these systems. As a member of this class, we investigated the uptake of pyrene into myristate-LDH. Because it is so hydrophobic, we find from isotherms that log K (K-partition coefficient) of pyrene to be 5.0, comparable to the octanol-water partition coefficient of 5.18. We also confirmed that pyrene is dispersed in the fatty acid part of the interlayer from its emission spectrum, shown below.

Emission spectra

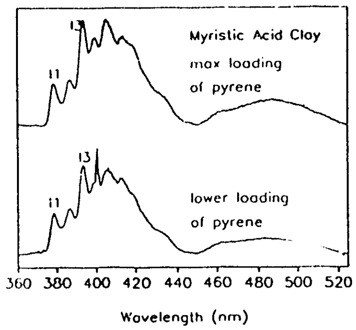

Lifetime

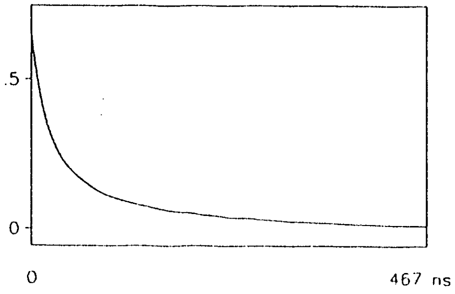

The ratio of peaks I/III is 0.4, comparable to that in hexane. If pyrene was dispersed in the ethanol phase, then this ratio would have been 1.2. Aggregation effects are observed at high loadings as evidenced by the excimer emission band at 500 nm. The lifetime decay of the triplet state is also shown above. It cannot be fitted to a sigle exponential decay indicating a multlipicity of sites, and emission from excimer states. The analysis of these data are in progress.

Publications Acknowledged to Grant

1. P.K. Dutta, W. Turbeville, "Intrazeolitic Photoinduced Reactions Between $Ru(bpy)_3^{2+}$ and Methylviologen" J. Phys. Chem.
2. P.K. Dutta, M. Borja, "Fatty Acids in Layered Metal Hydroxides: Membrane-like Structure and Dynamics, J. Phys. Chem. 1992, 96, 5434
3. P.K. Dutta, W. Turbeville, "Zeolite Entrapped $Ru(bpy)_3^{2+}$: Intermolecular Structural and Dynamic Effects, J. Phys. Chem. 1992, 96, 5024
4. P.K. Dutta and W. Turbeville, Examination of the Solvent-Like Nautre of Zeolites Based on a Solvatochromic Indicator, J. Phys. Chem. 1991, 95, 4087
5. P.K. Dutta and M. Borja, Pulsed Laser Photolysis of $Fe(CO)_5$ in Na-Y Zeolite, Zeolites, 1992, 12, 142

APPENDIX

Reprints removed and cycled separately

DATE FILMED

2 / 4 / 93